Article:
Pick, Lisa, Oehme, Vivien, Hartmann, Julia et al. (4 more authors) (2024) SilE-R and SilE-S - DABB Proteins Catalyzing Enantiospecific Hydrolysis of Organosilyl Ethers. Angewandte Chemie International Edition. ISSN 1433-7851

https://doi.org/10.1002/anie.202404105

How to cite: Angew. Chem. Int. Ed. 2024, e202404105
doi.org/10.1002/anie.202404105

Biocatalysis Very Important Paper

SilE-R and SilE-S—DABB Proteins Catalying Enantiospecific Hydrolysis of Organosilyl Ethers

Lisa M. Pick, Viviane Oehme, Julia Hartmann, Jessica Wenzlaff, Qingyun Tang, Gideon Grogan, and Marion B. Ansorge-Schumacher**

Abstract: Silyl ethers fulfil a fundamental role in synthetic organic chemistry as protecting groups and their selective cleavage is an important factor in their application. We present here for the first time two enzymes, SilE–R and SilE–S, which are able to hydrolyse silyl ethers. They belong to the stress-response dimeric A/B barrel domain (DABB) family and are able to cleave the Si–O bond with opposite enantiopreference. Silyl ethers containing aromatic, cyclic or aliphatic alcohols and, depending on the alcohol moiety, silyl functions as large as TBDMS are accepted. The X-ray crystal structure of SilE–R, determined to a resolution of 1.98 Å, in combination with mutational studies, revealed an active site featuring two histidine residues, H8 and H79, which likely act synergistically as nucleophile and Brønsted base in the hydrolytic mechanism, which has not previously been described for enzymes. Although the natural function of SilE–R and SilE–S is unknown, we propose that these 'silyl etherases' may have significant potential for synthetic applications.

Introduction

Environmentally friendly, sustainable and highly selective catalysts are crucial to the future of modern chemistry. In addition, the production of enantiomerically pure biologically active substances is of great importance as usually, only one enantiomer shows the desired biological effect, while the non-active enantiomer may cause adverse effects.[1]

[*] L. M. Pick, V. Oehme, J. Hartmann, J. Wenzlaff, Prof. Dr. M. B. Ansorge-Schumacher
Professur für Molekulare Biotechnologie
Technische Universität Dresden
01062 Dresden, Germany
E-mail: marion.ansorge@tu-dresden.de
Dr. Q. Tang, Prof. Dr. G. Grogan
Department of Chemistry
University of York
Heslington, York, YO10 5DD UK
E-mail: gideon.grogan@york.ac.uk

Enzymes fulfil these requirements to a high degree. They have therefore been the focus of attention for some time and are being utilised in synthetic organic chemistry up to industrial scale.[2] Hydrolases in particular have shown remarkable success and are now routinely used to produce glucose, biofuels, acrylamide or beta-lactam antibiotics.[3] In addition, the hydrolase-catalysed kinetic resolution of racemic alcohols for the production of active pharmaceutical ingredients (APIs) is well established, especially the synthesis of esters and amides with lipases.[1b,2b,4]

A reaction that has not previously been accessible with lipases or other enzymes to date, is the cleavage of silyl ethers.[5] Organosilyl ethers are the most commonly used protective group to prevent hydroxyl functions from modification during the chemical synthesis of complex molecules.[6] Recently, they have also become increasingly interesting for pharmaceutical applications and prodrug design due to their different chemical properties, compared to traditional carbon-containing analogs. These include higher lipophilicity resulting in increased cellular uptake, increased resistance to proteolytic degradation, no known intrinsic toxicity of the silicon and a distinct stability profile of the silyl ether linkages.[7]

Silyl ethers (also known as alkyloxysilanes) are chemical compounds that contain a silicon atom and an alkoxy group that are linked together by an atomic bond. The silicon atom is substituted with three alkyl or aryl residues as illustrated in Scheme 1.

The bulkiness of the alkyl residues determines the stability of the silyl ether bond: The more bulky the substituents are, the more stable is the bond.[6] Formation and cleavage of the silyl ether bond are generally achieved by the use of acids, bases and fluoride and these methods are of course not generally stereospecific.[6] However, the stereospecific cleavage or formation of silyl ethers could significantly increase their utility in complex chemical synthesis. It could also be useful for the production of pharmaceutically active organosilicons. Thus, considerable

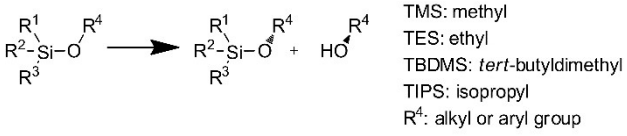

Scheme 1. Structure of silyl ethers.

efforts have been made in recent years to achieve stereospecific racemic resolution of silyl ethers using chemocatalysts and enzymes. Nevertheless, the task remains challenging.[2a,8]

For a long time it was thought that lipases might be able to catalyse the hydrolysis of silyl ethers because of the similarity of the silyl ether bond to the carboxylic acid ester bond.[9] However, we have recently shown that the sometimes observed (low) hydrolytic and condensation activity towards trimethylsilyl-protected alcohols is only due to non-specific interactions with the relevant protein.[5] Existing reports on enzymatic action towards silicon-containing compounds have focused mainly on silica deposition and condensation. In particular, proteins isolated from marine sponges and diatoms are known to build up very complex biosilica structures from inorganic silica.[10] It has been shown that this is at least partly controlled by structured networks of polypeptides containing long-chain polyamines and clusters of acidic and basic amino acids.[11] Glassin, a histidine-rich protein from marine sponges, was shown to rapidly accelerate silica polycondensation.[12] Very recently, Sarai *et al.* identified siloxane oxidase activity by some variants of cytochrome P450 enabling the breakage of Si–C-bond, highlighting the potential of directed evolution in the breakdown of non-natural organosilicon compounds.[13] Regarding silyl ethers, silicatein α, an enzyme isolated from marine sponges, has been shown to condense not only silica but also silyl ether bonds. Its mechanism of action was thought to act via a catalytic triad consisting of serine, histidine and asparagine including a nucleophilic attack on the Si atom by serine supported by hydrogen bonding to histidine.[14] However, there has been some debate over the mechanism of action and in the only available crystal structure the distance between Ser and His is beyond hydrogen bonding.[15] Some lines of evidence suggest that successful hydrolysis of silyl ethers may require the presence of catalytically active histidines: A computational study by Manville *et al.* on the enantioselective silylation of methanol showed that two *N*-methylimidazoles were involved in the silylation of methanol by TBDMSCl.[8b] While one was responsible for nucleophilic activation by forming a strongly electrophilic silyl intermediate, the other increased the nucleophilicity of methanol by acting as a Brønsted base. In addition, it has been shown that the attachment of a histidine tag to proteins leads to catalysts capable of the non-specific hydrolysis of silyl ethers.[16] These studies suggest that the search for an enzyme capable of silyl ether hydrolysis might consider proteins with suitably positioned His residues in a substrate binding cavity.

In this paper, we present for the first time two enzymes that are truly capable of catalysing the cleavage of silyl ether bonds. These enzymes, SilE–R and SilE–S, accept a range of silyl ether substrates and are also capable of acting stereospecifically. Rational design has even resulted in a variant able to hydrolyse an ether of the widely used, sterically demanding silyl protecting group *tert*-butyldimethylsilyl (TBDMS). Using a combination of the crystal structure of SilE–R with mutation and docking studies, candidates for the catalytically active residues have been proposed, and the active site determinants of enantiospecificity have been identified. This has permitted us to propose a reaction mechanism for silyl ether hydrolysis. These results identify SilE–R and SilE–S as new members of the DABB family with a novel 'silyl etherase' activity.

Results and Discussion

Novel Enzymes for Silyl Ether Cleavage

Silyl ethers are not known to occur naturally. Therefore, screening silyl ether-rich environments for enzymes that degrade them was not an option and we instead looked for enzymes that might display promiscuous silyl etherase activity. Based on the assumption described above that the specific hydrolysis of silyl ethers may be effected by catalytically active histidine residues in a putative active site, we chose phospholipase D (PLD) as promising target. PLD is a phosphodiesterase, the catalytic mechanism of which is based on a ping-pong mechanism involving two histidines acting on the phosphoester bond, each of which can be deprotonated by an adjacent aspartate.[17] Two commercially available PLD preparations from cabbage and *Streptomyces* sp. were tested for the enantiospecific hydrolysis of trimethylsilyl-protected 1-phenylethanol (**1**, Scheme 2).

In line with our expectations, the PLD preparation from cabbage indeed showed the ability to hydrolyse **1**. The activity showed a preference for the (*R*)-enantiomer of the racemic silyl ether (Supporting Information, Figure S1). We isolated PLD directly from cabbage and the extract was fractionated using blue native gel electrophoresis (Figure 1). The most prominent band from the analysis corresponded to the molecular weight of PLD, at approximately 87 kDa,[18] but the protein extracted from this showed no activity towards substrate **1**.

The ability to catalyse the enantiospecific cleavage of **1** was actually detected in a protein with a much lower molecular weight of around 20 kDa (Figure 1). Sequencing of the band identified the corresponding protein as an unknown 12.4 kDa plant stress response dimeric alpha/beta-barrel domain (DABB) family protein. Two proteins from cabbage with Uniprot accession numbers M4DUK5 and M4CDZ1 were matched to the unknown protein from the blue native PAGE and we named them SilE–S and SilE–R, respectively (SilE as a general abbreviation for 'silyl etherase'; the amino acid sequences of both proteins are given in the Supporting Information Figure S2). SilE–R had a sequence coverage of 99 % with the unknown blue native

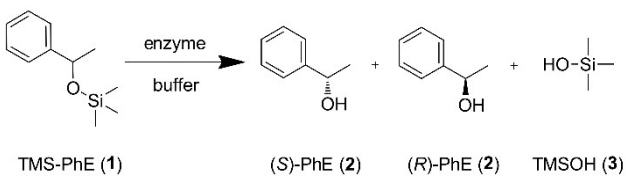

Scheme 2. Hydrolysis of TMS-protected 1-phenylethanol.

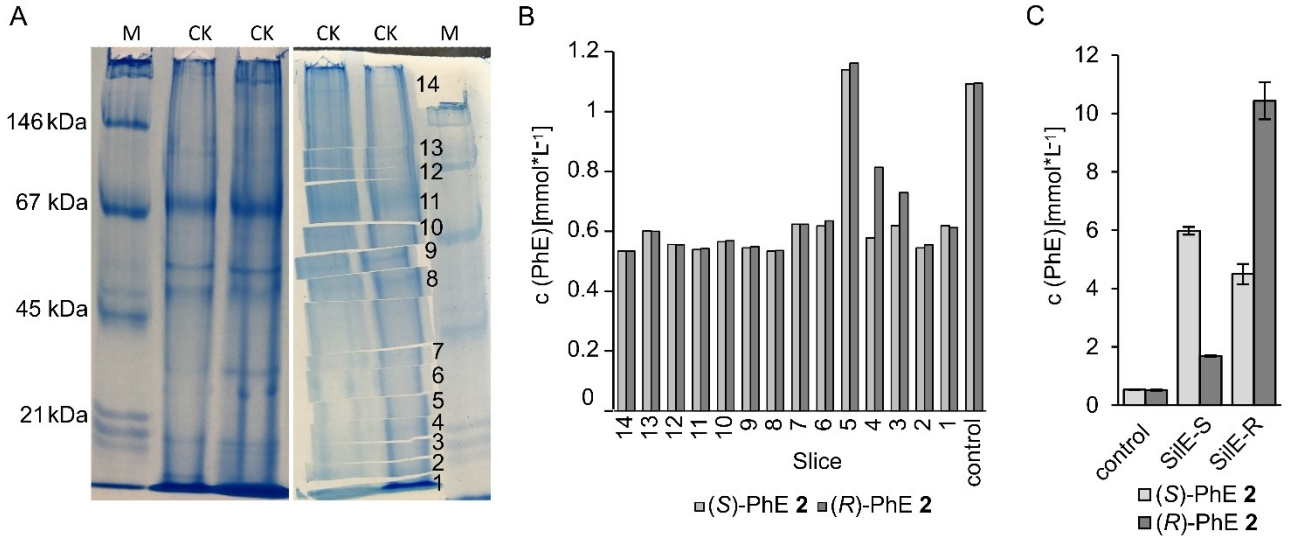

Figure 1. Identification of enzymes for silyl ether cleavage from purified cabbage extracts. A) Blue native PAGE of purified cabbage extract after heat precipitation at 55 °C, acetone precipitation and Ca^{2+}-dependent hydrophobic interaction chromatography. The gel was cut in half, the left half was stained with colloidal blue silver stain, the other half was left untreated. The untreated gel was sliced for further activity assays. B) 1-Phenylethanol (PhE) concentration from hydrolysis of 10 mmol*L^{-1} substrate **1** through untreated blue native side bands shown in A). Gel slices were minced and incubated with substrate in buffer (Tris-HCl, 50 mmol*L^{-1}, pH 8) for 24 h at room temperature. Samples were extracted 1 : 1 with iso-hexane for further analysis by GC. C) PhE concentration from hydrolysis of 25 mmol*L^{-1} substrate **1** by Strep-purified SilE–S and SilE–R in buffer (Tris-HCl, 50 mmol*L^{-1}, pH 8) after 24 h at room temperature. Samples were extracted 1 : 1 with iso-hexane for further analysis by GC. Error bars indicate standard deviations of independent triplicates. CK = purified Chinese cabbage extract; M = size standard; *(S)*/*(R)*-PhE = *(S)*-/*(R)*-1-phenylethanol; control = buffer and substrate only.

PAGE protein, whereas SilE–S had a coverage of 61 %. PDB entry 1RJJ, a protein of unknown function from *Arabidopsis thaliana*, shares 88 % sequence identity with SilE–R.[19] In addition, many proteins similar to SilE–R and SilE–S were found in databases, but mostly as predicted proteins with no known function. Enzymatic activity has not yet been described for any of the proteins or other proteins of the structural family such as HS1[20] and DABB1[21] from *Arabidopsis thaliana* and SP1 from *Populus tremula*.[22] They have also not yet been associated with silicate chemistry.

The genes encoding SilE–R and SilE–S were expressed in *E. coli* and purified (SI, Figure S3). Gas-chromatography assays demonstrated their ability to hydrolyse **1** (Figure 1C). It can be excluded that this activity is due to the modification of the proteins with a purification tag since the Strep tag was used. Unlike the His tag, the Strep tag does not have the ability to cleave silyl ethers unspecifically.[5,23] Including the Strep tag and a small linker between tag and protein, recombinant SilE–R and SilE–S had a theoretical size of 13.8 kDa and 13.9 kDa, respectively (SI, Figure S3). Interestingly, only SilE–R showed (*R*)-specificity towards **1**, as observed for the protein extracted from cabbage. SilE–S showed a clear preference for the (*S*)-enantiomer (Figure 1C). Hence either both proteins, or only SilE–R, could have been present in the cabbage extract. As neither SilE–S nor SilE–R had previously been ascribed an enzymatic function, we propose them as new members of the DABB family with 'silyl etherase' activity.

Biochemical Properties

SilE–R and SilE–S were both highly stable at moderate temperatures, but the activity decreased after a few hours at 50 °C for SilE–S and at 60 °C for SilE–R. At higher temperatures, both enzymes lost their activity within minutes (SI, Figure S4).

Both enzymes, SilE–R and SilE–S, showed good stability in the presence of 10 % (v/v) water-miscible organic solvents like DMSO, DMF, MeOH and MeCN (SI, Figure S5).

Addition of $MgSO_4$, $MgCl_2$, H_3BO_3, $NaSeO_3$, Na_2MoO_4, $NiCl_2$, $CuCl_2$, $ZnSO_4$, $CaCl_2$, $MnCl_2$, $FeCl_3$ and $FeCl_2$ at concentrations of 1 and 10 mmol*L^{-1}, respectively, or NH_4Cl at concentrations of 10 and 100 mmol*L^{-1}, respectively, to the reaction had no beneficial effect on the activity of SilE–R or SilE–S. $ZnSO_4$ and $CuCl_2$ significantly inhibited both enzymes (SI, Table S1).

Substrate Acceptance

In an initial substrate screen, both SilE–R and SilE–S demonstrated the ability to hydrolyse structurally different silyl ethers (Figure 2). SilE–R showed a clear preference for the (*R*)-enantiomer of all chiral compounds considered with an enantiomeric excess of 75 % for **1**; 66 % for **4** and 92 % for **9**, while SilE–S favoured the (*S*)-enantiomer showing an enantiomeric excess of 64 % for **1**, 55 % for **4** and 29 % for **9** (kinetic parameters are given in Table 1; see SI, Table S2A for % ee and S2B for yield, Figure S6, S7, S8, S10 for

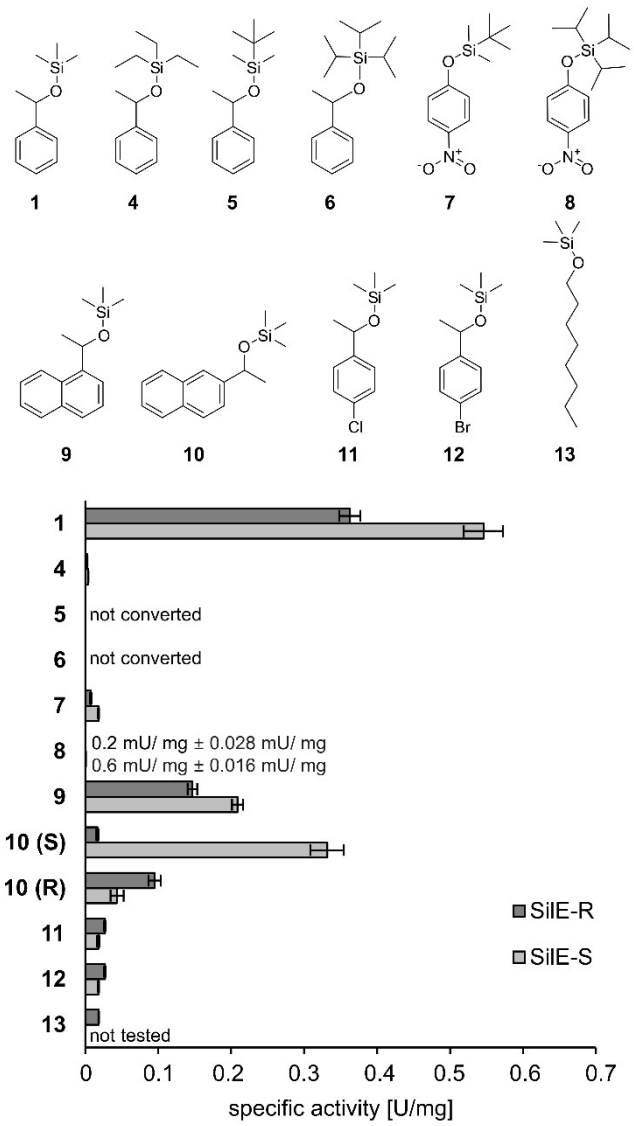

Figure 2. Substrates involved in the initial substrate screening and specific activity of SilEs for their hydrolysis. Bars represent the mean with standard deviation of independent triplicates. Racemic mixtures were used for all chiral substrates; S and R were not analysed separately due to lack of suitable analytical methods for some of the substrates, except for 1,2-naphthylethanol for which no racemic substrate was available.

chromatograms). To exclude unspecific hydrolysis of substrates with TMS and nitrophenol functions, which were observed with other enzymes in previous studies,[5,9c] control reactions were carried out with inactivated enzyme. Recognition of both the alcohol and the silanol moieties of the substrates by the enzymes was variable. **1** was converted with the highest activity by both enzymes. In addition to silylated 1-phenylethanols (**1**, **4**), *para*-halogenated substrates (**11** and **12**), bicyclic compounds (**9** and **10**) and nitrophenols (**7** and **8**) were also accepted. Furthermore, silylated aliphatic 1-octanol (**13**) was accepted, despite a high background hydrolysis (SI, Figure S15). In combination with 1-phenylethanol, the larger TES (**4**) group was also accepted instead of TMS. 1-phenylethanol silyl ethers with the TIPS (**6**) or TBDMS (**5**) group were not transformed. In contrast, it was possible to hydrolyse 4-nitrophenol silyl ethers with both of these protecting groups (**7** and **8**) (Figure 2; SI, Figure S6–S14).

The kinetic constants for SilE–R and SilE–S were determined using **1**, **4**, **7** and **10**. In general, the measured K_m values were surprisingly rather low (Table 1), indicating a high affinity of the proteins for the substrates. However, the k_{cat} values were also low. The specific activity followed the stability trend of the silyl ethers, as compounds with bulkier substituent derivatives were more stable[6] and exhibited lower k_{cat} values: The specific activity was higher towards **1** over **4** and for **7** over **8** (Figure 2).

Structure of SilE-R

In order to probe the molecular determinants of mechanism and stereospecificity in the enzymes the structure of SilE–R was determined by X-ray crystallography and refined to a resolution of 1.98 Å. The crystals were in space group $P3_221$ and featured two molecules in the asymmetric unit, constituting a dimer as observed in solution by SEC studies (SI, Figure S16). The SilE–R dimer was asymmetric, however, in that the 'B' subunit possessed an intact Strep tag that was absent from the 'A' subunit (SI Figure S17). Each monomer consists of a βαββααβ topology, in which all the β-strands form one β-sheet. The monomers dimerise at the β-sheets forming a barrel-like structure typical of plant stress-responsive alpha/beta-barrel domain-containing proteins (Figure 3A).

Dimeric alpha/beta barrel (DABB) proteins[24] have been reported to have a variety of functions, including as stress proteins[22b] but also as hydroxynitrile lyases,[25] polyketide cyclases[26] and cofactor-independent oxygenases.[27] A search for proteins of similar fold using the DALI server and the monomer of SilE–R revealed the closest structural overlap (SI, Figure S18) with the 'boiling stable' stress protein SP1 from *Populus tremula* (1TR0, 30 % sequence id; 1.4 Å rmsd over 98 Cα atoms)[22b] but also a hydroxynitrile lyase (HNL) from *Passiflora edulis* (5Y02, 30 % sequence id; 1.7 Å rmsd over 99 Cα atoms)[25] and the olivetolic acid cyclase (OAC) from *Cannabis sativa* (5B09, 33 % sequence id; 1.6 Å rmsd over 96 Cα atoms).[26] Analysis of the surface of the SilE–R structure revealed a deep hydrophobic pocket formed by the β-sheet and α-helices of each monomer (Figure 3B–D), partially covered by a loop from the other dimerising monomer. This region served as the active site in both HNL and OAC.[25–26] Active site residues shared with the HNL included H8 (5Y02 H8), F64 (F68), F73 (F77) and F86 (F90). However, there were also differences, including F14 (Y14), L27 (Y30), F40 (W43), F60 (Y64), M62 (S66), T87 (F91), H79 (A83), S83 (A87) and D97 (N101), which either removed or added catalytic potential at different points in the active site (SI, Figure S19). Interestingly, H8, the catalytic acid-base residue in the HNL was conserved, although its dyad partner N101 was replaced by D97 in SilE–R.[25] Of the other residues in the HNL identified as

Table 1: Kinetic parameters for SilE–R and SilE–S catalysed silyl ether hydrolysis.

Substrate		SilE-S K_m (mmol*dm^{-3})	SilE-S k_{cat} (s^{-1})	SilE-S k_{cat}/K_m s^{-1}/(mmol*dm^{-3}))	SilE–R K_m (mmol*dm^{-3})	SilE–R k_{cat} (s^{-1})	SilE–R k_{cat}/K_m s^{-1}/(mmol*dm^{-3}))
1	S	0.099 ± 0.016	0.09 ± 0.003	0.91	0.224 ± 0.036	0.023 ± 0.001	0.1
	R	0.137 ± 0.026	0.024 ± 0.001	0.18	0.05 ± 0.02	0.126 ± 0.011	2.5
4	S	0.004 ± 0.001	0.0008 ± 4*10^{-5}	0.2	0.017 ± 0.004	0.0001 ± 5.6*10^{-6}	0.006
	R	0.01 ± 2.9*10^{-3}	0.0001 ± 5.7*10^{-6}	0.01	0.009 ± 0.004	0.0014 ± 1.2 *10^{-4}	0.16
10	S	0.03 ± 0.007	0.076 ± 0.003	2.5	0.056 ± 0.014	0.0038 ± 0.0003	0.07
	R	0.08 ± 0.026	0.01 ± 0.0008	0.13	0.032 ± 0.011	0.024 ± 0.002	0.75
7		0.007 ± 0.001	0.0009 ± 3.4*10^{-5}	0.13	0.006 ± 0.002	0.0005 ± 3.6 *10^{-5}	0.08

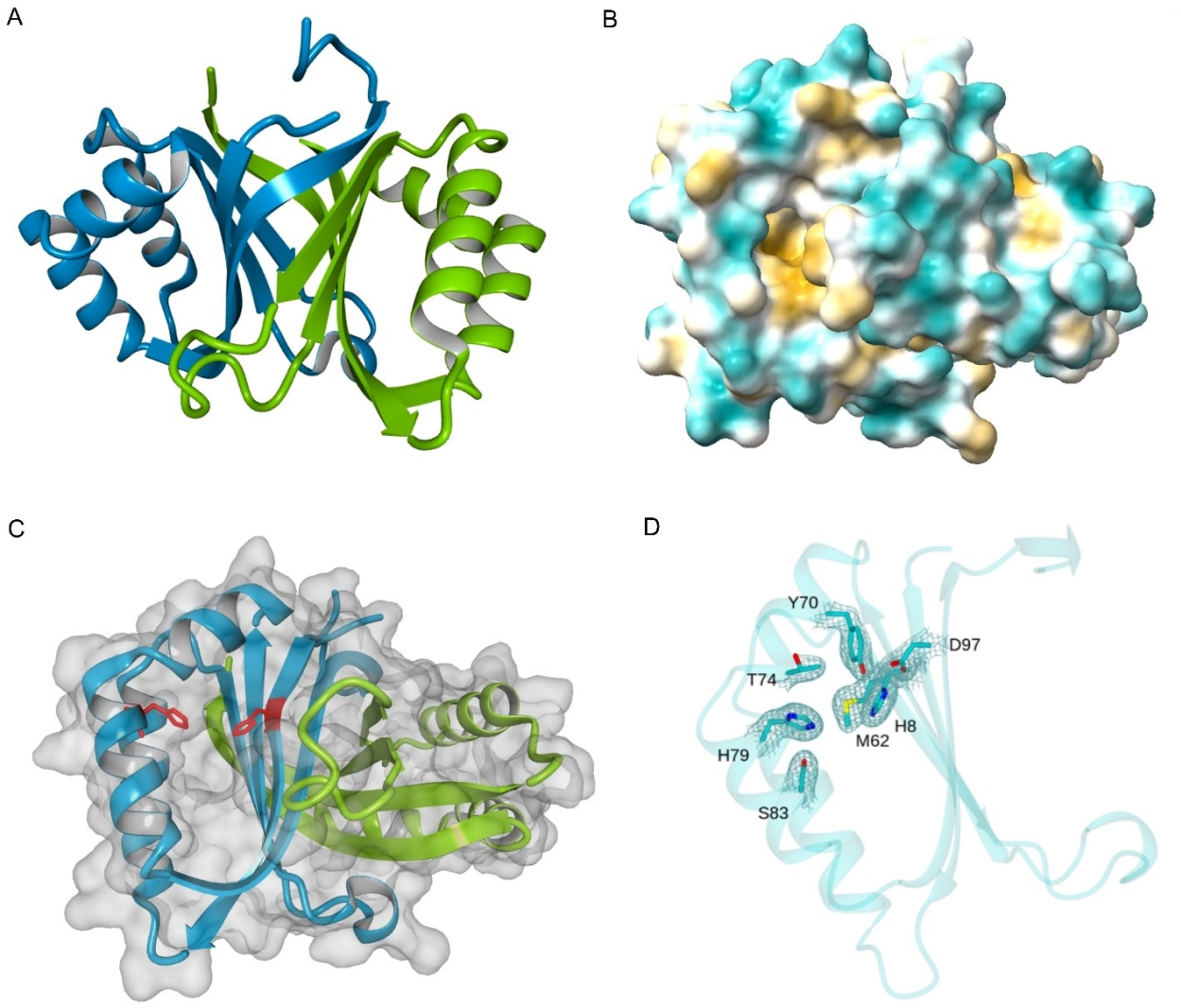

Figure 3. Crystal structure of SilE–R. A) The crystal structure is composed of two monomers, shown in blue and green, forming a barrel-like structure. B) The surface shows a deep hydrophobic pocket (hydrophobic residues are shown in yellow, while turquoise represents hydrophilic regions). C) This pocket is formed by the beta sheet and alpha helices and contains two histidine residues. D) Active site of monomer of SilE–R showing side-chains of residues mutated in the study. The electron density corresponds to the refined $2F_o–F_c$ map at a level of 1σ.

important for the mechanism, Y30 is replaced by L27, R56 by L52 and E54 is conserved as E50, although this does not project into the active site of SilE–R in the determined structure.

OAC catalyses the aldol cyclisation of a linear pentyl tetra-β-ketide CoA to give olivetolic acid as the product.[26] The similarity of SilE–R to OAC (5B09) is interesting, because, in addition to the conservation of H8 and its dyad partner D97 (H5 and D95 in 5B09), the other histidine H79 (H78) is also conserved (Figure 3C, SI, Figure S19) although it is the latter that is proposed to make the catalytic contribution as acid-base in OAC.[26]

Catalytic Mechanism

From the structure of SilE–R, we identified H8, M62, Y70, T74, H79, S83 and D97 as residues within the hydrophobic pocket that could potentially be involved in the catalytic cleavage of silyl ethers. In order to investigate their putative roles in catalysis, we first mutated these residues in SilE–R to alanine and tested the activity of the resulting variants against the cleavage of **1**. We then repeated this for SilE–S with the amino acids, the mutation of which had an effect on activity when mutated to alanine in SilE–R. These experiments confirmed that H8, H79, D97, M62 and Y70 were all catalytically significant (Figure 4, SI, Figure S20). Single mutations of Y70 and M62 to A reduced the total activity in both enzymes. Mutations of H8, H79 and D97 to A extinguished the activity of SilE–S, but for SilE–R, only the activity towards the (*R*)-enantiomer was abolished, while some (*S*)-product was still formed. Thus, the enantiospecificity of SilE–R was reversed. To completely inactivate SilE–R, it was necessary to create the double mutant H8A/Y70A. These results point to important roles for catalysis by H8 and H79 in both SilE–R and SilE–S, with a possible additional role for Y70 in some instances that has yet to be determined. The double mutant H8A/Y70A, as well as the H8A mutant of SilE–S, were further used as the negative controls in all assays to distinguish between enzyme-catalysed hydrolysis and non-specific hydrolysis by the protein moieties as described in the literature.[5]

The acidic and basic contributions of the residues, especially with respect to the two histidines H8 and H79, were estimated using PropKa[28] using the crystal structure of SilE–R. Interestingly, H79 appears to be a strong acid, mainly due to desolvation effects (see SI, Table S3, for detailed results), while H8 is more neutral, hydrogen bonding to acidic D97, which itself is hydrogen bonding to basic Y70. These results suggest that H79 acts as an acid, while H8 probably acts as a base. Based on these results, we propose two possible mechanisms for silyl ether cleavage by SilE–R and SilE–S.

The first mechanism ("nucleophile-covalent") involves roles in acid-base catalysis for H8 and nucleophilic attack by H79 respectively (Figure 5A). Previous studies by Manville *et al.* used a chemocatalyst containing 2-*N*-methylimidazole for enantioselective silylation.[8b] They showed that two molecules of this catalyst acted synergistically, one as a Brønsted base, while the other acted as a nucleophilic promoter to activate the silyl species.[8b] If this mechanism was transposed to SilE–R and SilE–S, H79 would directly attack the silicon and assume the role of the nucleophile, forming a silyl enzyme intermediate, while H8 would act as a Brønsted base, transferring a proton to the silyl ether linkage and releasing the alcohol moiety from the enzyme. The deprotonated H8 would then activate a water molecule, creating a hydroxyl which is transferred to the silyl moiety, releasing the silanol from the enzyme. To aid acid-base catalysis, H8 forms a dyad with D97, which in turn forms a hydrogen bond with Y70. M62 would have a role in electrostatic stabilization of the positively charged histidines.[29] Furthermore, following the need to create a double mutant H8A/Y70A to completely inactivate the SilE–R, Y70 might be able to take over the function of H8

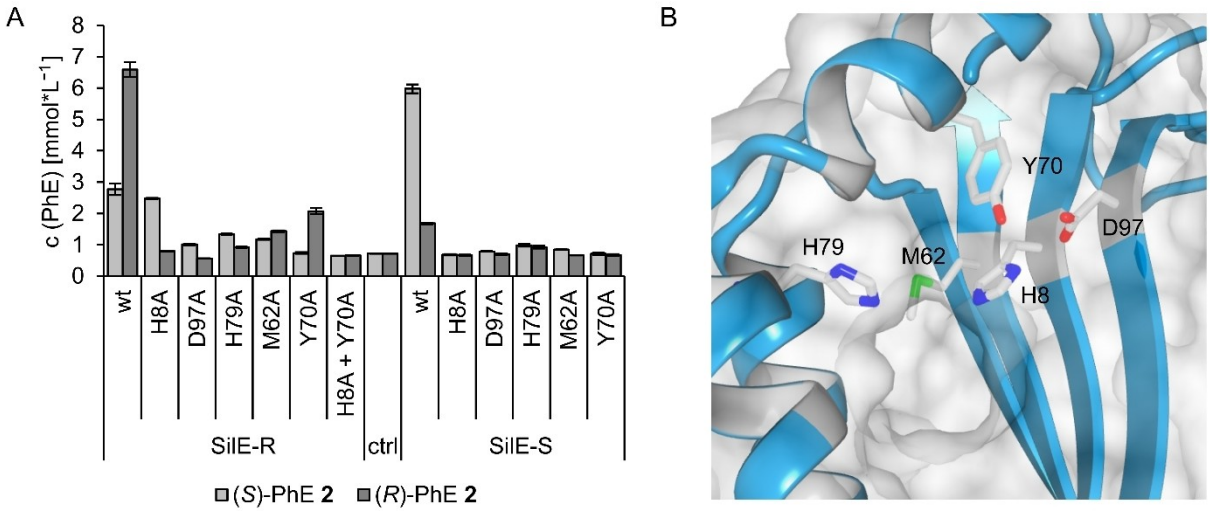

Figure 4. Catalytically active residues within the hydrophobic pocket of SilE–R and SilE–S. A) Activity assay of alanine-mutants. Shown is the mean product concentration with standard deviation of three independent samples. For the assay, 0.01 mmol*L^{-1} Strep-purified mutants, 50 mmol*L^{-1} Tris-HCl pH 8 and 20 mmol*L^{-1} substrate **1** were incubated at room temperature and 400 rpm for 24 h. Samples were extracted 1 : 1 with isohexane for gas chromatography. "ctrl" = buffer and substrate only. B) Position of catalytically active residues in SilE–R.

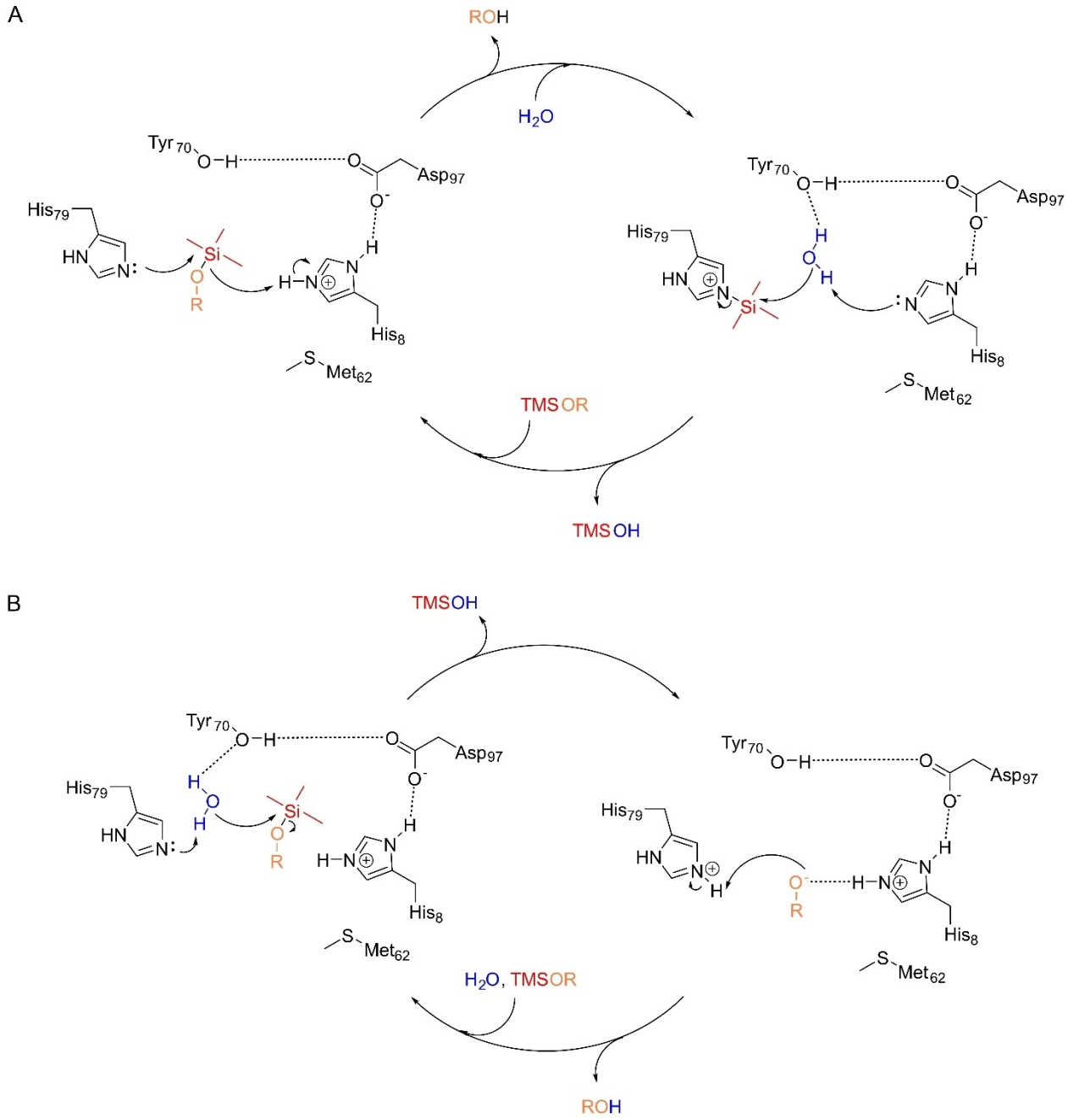

Figure 5. Possible reaction mechanisms for cleavage of silyl ethers by SilE–R and SilE–S. A) Mechanism 1: "nucleophile-covalent". H79 directly attacks the silicon while H8 transfers a proton to the silyl ether bond, releasing the alcohol moiety from the enzyme. The deprotonated H8 deprotonates a water molecule creating a hydroxyl, which is transferred to the silyl moiety releasing the silanol from the enzyme. M62 temporarily stabilises the positively charged histidines electrostatically. B) Mechanism 2: "acid-base". H79 drives a nucleophilic attack on a water molecule forming a hydroxyl. This hydroxyl attacks the silyl moiety while H8 transfers a proton to the ether oxygen, cleaving the bond and releasing the newly formed silanol. To assist this, H8 forms a dyad with D97. M62 further enables this mechanism by transiently electrostatically stabilising the positive charge of H8. The proton from the original water molecule still bound to H79 is now transferred to the alcohol, which is also released from the enzyme.

as the base transferring a proton on the silyl ether linkage and activating the water molecule.

The second putative mechanism ("acid-base") is based on a classical acid-base-catalysed hydrolysis involving water as nucleophile (Figure 5B). H79 first activates a water molecule for attack at the silyl moiety while H8 transfers a proton to the ether oxygen, cleaving the bond and releasing the newly formed silanol. M62 would again further enable this mechanism by transient electrostatic stabilisation of the positive charge of H8.[29] Either a proton from another water

molecule enters the active site, or the proton from the original water molecule still bound to H79 is transferred to the alcohol, also releasing the alcohol from the enzyme (Figure 5B). This second mechanism is based on the assumption that the silyl moiety is oriented outside the binding pocket.

Attempts to obtain a substrate-bound crystal structure of SilE–R were unsuccessful, so, a docking study was performed using Autodock 4.[30] Interestingly, docking with **1** strongly suggested that the silyl moiety is orientated towards the inside and the alcohol toward the outside of the active site supporting the first nucleophile-covalent mechanism (Figure 6). While for the (*R*)- enantiomer, four competent poses were identified (only the two best are shown), only two could be found for the (*S*)-enantiomer with binding statistics being superior for the (*R*)-enantiomer.

These findings support the (*R*)-preference detected in experiments (Figure 1C, Table 1; SI, Figure S6, S7, S8, S10 and Table S2).

SilE–R and SilE–S accepted all alcohols tested in the initial substrate screening, but did not convert the large substrate **5** (Figure 2). This further supports a binding of the silyl group oriented within the binding pocket, i.e. the first mechanism proposed. Interestingly, hydroxynitrile lyase from *Passiflora edulis*[25] and olivetolic acid cyclase,[26] which share structural features with SilE–R and SilE–S, also bind their aromatic substrates with the aromatic ring oriented towards the binding site entrance (PDB: 5Y02 for hydroxynitrile lyase from *P. edulis* in complex with mandelonitrile and PBD: 5B09 for olivetolic acid cyclase in complex with olivetolic acid). However, HNL has a different catalytic site as it does not contain H79, D97, M62 or Y70 and D97 is replaced by N. OAC contains H8, H79 and D97, but not M62 and Y70. It remains questionable therefore whether OAC might hydrolyse silyl ethers, given the absence of the catalytically important residues M62 and Y70.

Parallels to the first proposed mechanism of histidine-catalysed silyl ether hydrolysis (Figure 5A) can also be found in phospholipase D. PLD has two histidines in its active site to hydrolyse the phosphodiester bond of phospholipids. One histidine acts a nucleophile to attack the phosphate to form a phosphatidyl enzyme intermediate, while the other transfers a proton to the alcohol moiety, releasing the alcohol. In the next step, this histidine takes a proton from water, while the hydroxyl from the water releases the phosphatidic acid from the enzyme.[17] However, in contrast to SilE–R and SilE–S, in PLD, both histidines are supported by an aspartate.

The docking, in combination with a comparison with structurally close enzymes' binding modes and mechanisms strongly support direct attack of H79 on the silicon atom, as shown in Figure 5A, similar to the synthetic catalysts used by Manville *et al.* (2013).[8b] However, we cannot completely exclude the second, non-covalent mechanism with a nucleophilic attack by an activated water molecule as the first step.

Origin of Enantiospecificity

The amino acid sequences of SilE–R and SilE–S differ by only eleven out of 111 amino acids (for sequence alignment see SI, Figure S2). By individually replacing these eleven amino acids in SilE–R with the corresponding amino acids in SilE–S using site-directed mutagenesis, we were able to identify position 27, where SilE–R and SIlE–S contain leucine and serine respectively, as responsible for the different enantiopreference of the two enzymes (Figure 7A). The exchange of these amino acids leads to the opposite enantiopreference in both enzymes (Figure 7B, for kinetic parameters see Supporting Information Table S4). Saturation mutagenesis of position 27 slightly improved the (*R*)-specificity to over 60 % ee when it was a larger amino acid (Trp, Tyr, Phe) and the (*S*)-specificity to 89 % ee when it was smaller (Gly) (Figure 7C, Supporting Information Figure S6 and S7). The structurally related enzyme HNL from *P. edulis* also shows (*R*)-specificity for its substrate mandelonitrile.[25] In agreement with our results, this HNL has a tyrosine at position 30, which corresponds to position 27 in SilE–R.

Extended Substrate Range

Alanine scanning of six amino acids (V10, V95, F86, S83, I93, L27) in the active site of SilE–R gave two variants, V10A and L27A, with a substrate acceptance that now

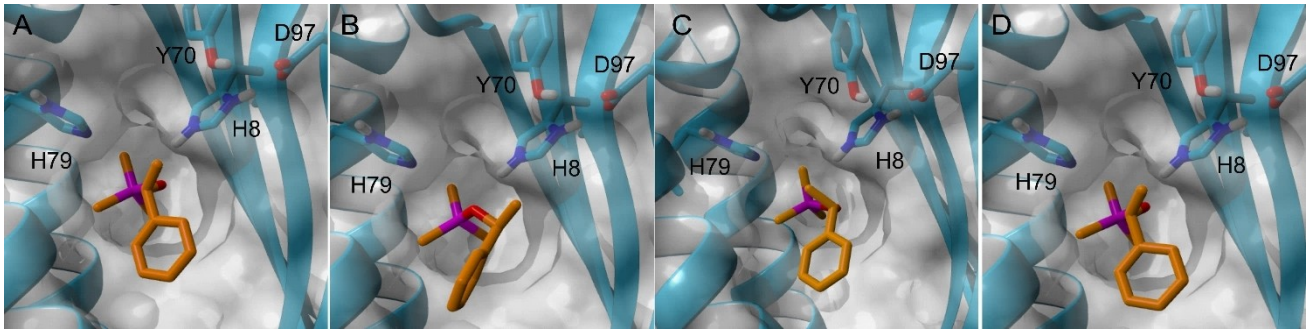

Figure 6. Figure S18: SilE–R with TMS-(*R*)-1-phenylethanol **1** (A + B), TMS-(*S*)-1-phenylethanol **1** (D + C). For A–D a reaction mechanism as shown in Figure 5A is assumed. Docking was performed with Autodock 4.[30] Binding energies (kcal*mol^{-1}): A) −5.28, B) −5.22, C) −5.19, D) −4.53. Distances H8-Hε to ether-O in Å: A) 2.23, B) 1.88, C) 2.7, D) 2.69. Distances H79-Nε to Si in Å: A) 3.68, B) 3.5, C) 4.09, D) 3.46.

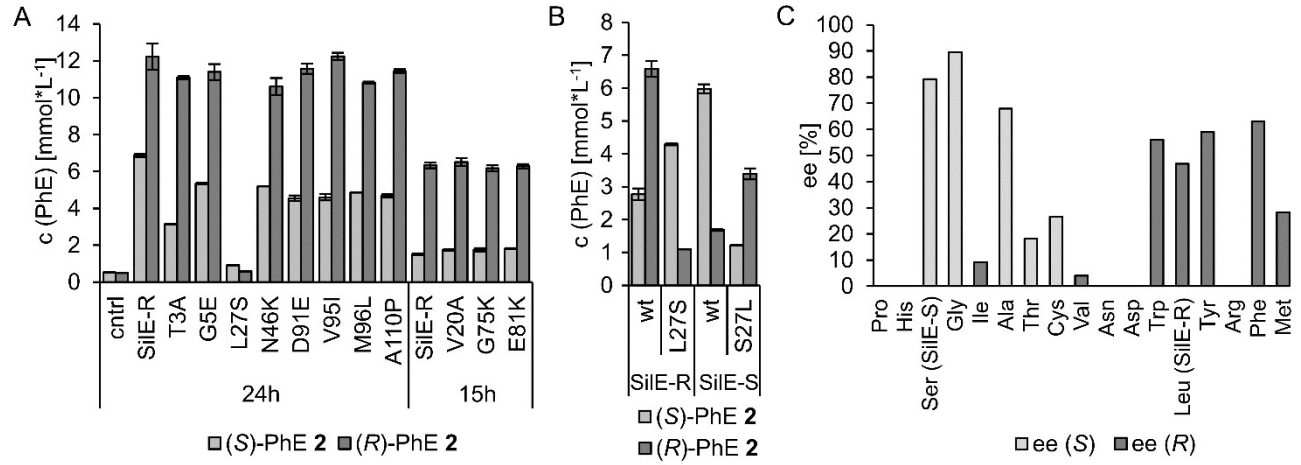

Figure 7. A) Hydrolysis of **1** by mutants created by replacing all SilE–R amino acids that were different in SilE–S with amino acids of SilE–S. 1 mL of culture (OD = 2) was harvested, the pellet was resuspended in 50 mmol*L^{-1} Tris-HCl pH 8, the cell suspension was sonicated to disrupt the cells, centrifuged at 17,000xg and the clear supernatant was used for activity assay. For the assay, 1 µL substrate (**1**) was added to 200 µL clear supernatant (final substrate concentration was 20 mmol*L^{-1}) and incubated at room temperature, 400 rpm for 24 or 15 h before extraction 1 : 1 with isohexane and measured by gas chromatography to determine the product concentration. "cntrl" = buffer and substrate only. B) Opposite enantiopreference in hydrolysis of **1** by SilE–R and SilE–S and the corresponding L27S and S27 L mutants. For the hydrolysis assay, 20 mmol*L^{-1} substrate and 0.01 mmol*L^{-1} purified enzyme were incubated in 50 mmol*L^{-1} Tris-HCl pH 8 for 4 h at 400 rpm. Samples were extracted (1 : 1) with isohexane and measured by GC to determine product concentration. C) Enantiomeric excess generated during hydrolysis of **1** by mutants of SilE–R with the indicated amino acids at position 27. The assay was performed as in A). Bars represent the mean and error bars the standard deviation of triplicates. For the determination of ee [%], the means of the triplicates were used with the formula ((preferred product - inferior product)/total product)*100. For peak separation see Supporting Information, Figure S5 and S6.

included the bulky substrate **5** with a TBDMS group. The conversions with both enzymes were low, but clearly detectable (Figure 8A; SI, Figure S21). V10A showed (*R*)-enantiopreference like the wild-type enzyme, while L27A acted (*S*)-specifically. This matched our results on the influence of position 27 on the enantiopreference of the enzyme. Both amino acids, V10 and L27, are located quite deep inside the binding pocket, suggesting that the TBDMS group is bound inside the binding pocket with the alcohol residue exposed to the outside, as previously proposed. Docking of **5** inside the SilE–R-V10A variant, the SilE–R-L27A variant and the wild-type enzyme revealed a different positioning of the *tert*-butyl group within the binding pocket. It filled the additional space created by the replacement of V10 and L27 by the smaller amino acid alanine, whereas no competent position was identified for the wild-type enzyme (Figure 8B–D).

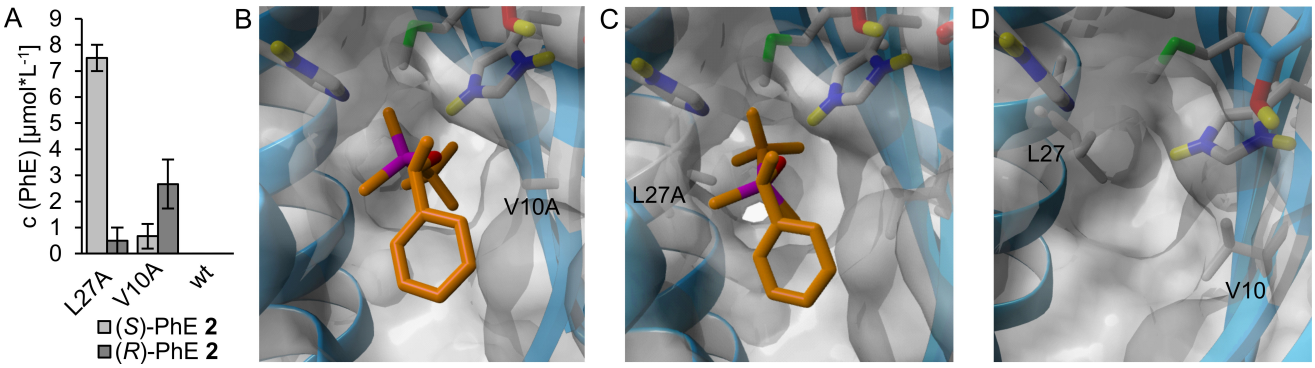

Figure 8. A) 1-Phenylethanol concentration from the hydrolysis of **5** by SilE–R L27A, SilE–R V10A and wild-type SilE–R (wt). The reaction was carried out with 1 mmol*L^{-1} substrate and 0.05 mmol*L^{-1} enzyme in 50 mmol*L^{-1} Tris-HCl pH 8 for 24 h at room temperature with shaking at 400 rpm. Samples were extracted with 1 : 1 isohexane for GC analysis. B–D) Docking of TBDMS-(*R*)-1-phenylethanol into SilE–R V10A (B) and SilE–R L27A (C). For wt SilE–R (D) no competent pose could be identified, whereas for both variants the binding sites show an orientation of the tert-butyl group towards the mutated amino acid (alanine), which gives more space than the wt amino acids (valine/leucine). Binding affinities according to Autodock 4 (kcal mol^{-1}): V10A: −4.94; L27A: −5.03.

Distribution in Nature

In addition to Chinese cabbage, we were also able to demonstrate enantiospecific hydrolytic activity towards substrate **1** by extracts of white cabbage (*Brassica oleracea* convar. *capitata* var. *alba*) and savoy cabbage (*Brassica oleracea* var. *sabauda L.*) as well as in the phylogenetically more distant leek (*Allium porrum*) (SI, Figure S22).

The natural function of the silyl etherases from cabbage or other potential producers remains enigmatic. We tested several other substrates including aromatic and aliphatic esters, various phosphoesters, an ether substrate, benzamide and hexaethyldisiloxane as well as the HNL substrate mandelonitrile,[25] but none was accepted as substrate by our silyl etherases (see SI, Table S5 for a complete list).

Conclusion

SilE–R and SilE–S are the first enzymes to be identified that have the ability to hydrolyse silyl ethers enantiospecifically. The reaction seems to be catalysed by an active site involving two histidine residues. This might confirm the expectations from earlier studies on silyl ether cleavage.[8b,15c] However, the catalysis seems likely to follow a mechanism not previously described for enzymes. This is indicated by the nature of the other amino acid residues involved in catalysis compared to the structurally close enzymes HNL and OAC as well as the mechanistically close enzyme PLD and the inability of SilE–R and SilE–S to cleave the substrates of other enzymes. We therefore propose that SilE–R and SilE–S might represent new members of the DABB family of proteins with 'silyl etherase' activity, for which the natural substrates have not yet been identified. We envisage that these enzymes may have valuable applications in the green and selective transformation of organosilanol substrates.

Supporting Information

The authors have cited additional references within the Supporting Information.[31]

Acknowledgements

This work was funded by Deutsche Forschungsgemeinschaft (DFG, German Research Foundation) within project 417423160. Q.T. was funded by grant EP/T01430X/1 from the UK Engineering and Physical Sciences Research Council (EPSRC). The authors thank Dr. M. Gentzel and K. Eismann of the Core Facility 'Mass Spectrometry & Proteomics', CMCB, Dresden University of Technology for protein sequencing and support. The Core Facility was generously supported by grants from European Regional Development Fund (ERDF/EFRE) (Contract #100232736) and the Deutsche Forschungsgemeinschaft (DFG) (INST 269/731-1613 FUGG). We also thank Mr Sam Hart and Dr Johan P. Turkenburg for assistance with X-ray data collection, and the Diamond Light Source Didcot UK for access to beamline I03 under proposal mx32736. Open Access funding enabled and organized by Projekt DEAL.

Conflict of Interest

The authors declare no conflict of interest.

Data Availability Statement

The data that support the findings of this study are available from the corresponding author upon reasonable request.

Keywords: biocatalysis · hydrolases · silyl ether · silyl etherases · enantiospecific hydrolysis

[1] a) E. Ariens, *Eur. J. Clin. Pharmacol.* **1984**, *26*, 663–668; b) R. N. Patel, *Bioorg. Med. Chem.* **2018**, *26*, 1252–1274.
[2] a) J. Seliger, M. Oestreich, *Chem. Eur. J.* **2019**, *25*, 9358–9365; b) H. Sun, H. Zhang, E. L. Ang, H. Zhao, *Bioorg. Med. Chem.* **2018**, *26*, 1275–1284.
[3] R. A. Sheldon, D. Brady, M. L. Bode, *Chem. Sci.* **2020**, *11*, 2587–2605.
[4] U. T. Bornscheuer, R. J. Kazlauskas, *Hydrolases in organic synthesis: regio-and stereoselective biotransformations*, John Wiley & Sons **2006**.
[5] L. M. Pick, J. Wenzlaff, M. Yousefi, M. D. Davari, M. B. Ansorge-Schumacher, *ChemBioChem* **2023**, *24*, e202300384.
[6] P. J. Kocienski, *Protecting Groups*, Georg Thieme Verlag **2005**.
[7] A. K. Franz, S. O. Wilson, *J. Med. Chem.* **2013**, *56*, 388–405.
[8] a) Y. Zhao, J. Rodrigo, A. H. Hoveyda, M. L. Snapper, *Nature* **2006**, *443*, 67–70; b) N. Manville, H. Alite, F. Haeffner, A. H. Hoveyda, M. L. Snapper, *Nat. Chem.* **2013**, *5*, 768–774.
[9] a) M. Therisod, *J. Organomet. Chem.* **1989**, *361*, C8–C10; b) A. R. Bassindale, K. F. Brandstadt, T. H. Lane, P. G. Taylor, *J. Inorg. Biochem.* **2003**, *96*, 401–406; c) A. Maraite, M. B. Ansorge-Schumacher, B. Ganchegui, W. Leitner, G. Grogan, *J. Mol. Catal.* **2009**, *56*, 24–28; d) V. Abbate, K. F. Brandstadt, P. G. Taylor, A. R. Bassindale, *Catalysts* **2013**, *3*, 27–35; e) H. Nishino, T. Mori, Y. Okahata, *Chem. Commun.* **2002**, 2684–2685; f) P. Brondani, M. Mittersteiner, M. Voigt, B. Klinkowski, D. Riva Scharf, P. de Jesus, *Synthesis* **2018**, *51*, 477–485.
[10] a) N. Kröger, R. Deutzmann, M. Sumper, *Science* **1999**, *286*, 1129–1132; b) S. Wenzl, R. Hett, P. Richthammer, M. Sumper, *Angew. Chem. Int. Ed.* **2008**, *47*, 1729–1732; c) A. Scheffel, N. Poulsen, S. Shian, N. Kröger, *Proc. Natl. Acad. Sci. USA* **2011**, *108*, 3175–3180; d) A. Kotzsch, P. Gröger, D. Pawolski, P. H. H. Bomans, N. A. J. M. Sommerdijk, M. Schlierf, N. Kröger, *BMC Biol.* **2017**, *15*, 65.
[11] D. Otzen, *Scientifica* **2012**, *2012*, 867562.
[12] K. Shimizu, T. Amano, M. R. Bari, J. C. Weaver, J. Arima, N. Mori, *Proc. Natl. Acad. Sci. USA* **2015**, *112*, 11449–11454.
[13] N. S. Sarai, T. J. Fulton, R. L. O'Meara, K. E. Johnston, S. Brinkmann-Chen, R. R. Maar, R. E. Tecklenburg, J. M. Roberts, J. C. T. Reddel, D. E. Katsoulis, F. H. Arnold, *Science* **2024**, *383*, 438–443.
[14] Y. Zhou, K. Shimizu, J. N. Cha, G. D. Stucky, D. E. Morse, *Angew. Chem. Int. Ed.* **1999**, *38*, 779–782.
[15] a) M. Fairhead, K. A. Johnson, T. Kowatz, S. A. McMahon, L. G. Carter, M. Oke, H. Liu, J. H. Naismith, C. F.

van der Walle, *Chem. Commun.* **2008**, 1765–1767; b) S. Görlich, A. J. Samuel, R. J. Best, R. Seidel, J. Vacelet, F. K. Leonarski, T. Tomizaki, B. Rellinghaus, D. Pohl, I. Zlotnikov, *Proc. Natl. Acad. Sci. USA* **2020**, *117*, 31088–31093; c) E. I. Sparkes, The University of Manchester **2019**.

[16] E. I. Sparkes, R. A. Kettles, C. S. Egedeuzu, N. L. Stephenson, S. A. Caslin, S. Y. Tabatabaei Dakhili, L. S. Wong, *Biomol.* **2020**, *10*, 1209.

[17] I. Leiros, S. McSweeney, E. Hough, *J. Mol. Biol.* **2004**, *339*, 805–820.

[18] R. Lambrecht, R. Ulbrich-Hofmann, *Biol. Chem.* **1992**, *373*, 81–88.

[19] G. Cornilescu, C. C. Cornilescu, Q. Zhao, R. O. Frederick, F. C. Peterson, S. Thao, J. L. Markley, *J. Biomol. NMR* **2004**, *29*, 387–390.

[20] S.-C. Park, J. R. Lee, S.-O. Shin, Y. Park, S. Y. Lee, K.-S. Hahm, *Biochem. Biophys. Res. Commun.* **2007**, *362*, 562–567.

[21] J. R. Lee, S. S. Lee, S.-C. Park, J. S. Kang, S. Y. Kim, K. O. Lee, S. Y. Lee, *Biochim. Biophys. Acta Proteins Proteomics* **2008**, *1784*, 1918–1923.

[22] a) W. X. Wang, D. Pelah, T. Alergand, O. Shoseyov, A. Altman, *Plant Physiol.* **2002**, *130*, 865–875; b) O. Dgany, A. Gonzalez, O. Sofer, W. Wang, G. Zolotnitsky, A. Wolf, Y. Shoham, A. Altman, S. G. Wolf, O. Shoseyov, O. Almog, *J. Biol. Chem.* **2004**, *279*, 51516–51523.

[23] E. I. Sparkes, C. S. Egedeuzu, B. Lias, R. Sung, S. A. Caslin, S. Y. Tabatabaei Dakhili, P. G. Taylor, P. Quayle, L. S. Wong, *Catalysts* **2021**, *11*, 879.

[24] M. Dastmalchi, *Plant J.* **2021**, *108*, 314–329.

[25] F. Motojima, A. Nuylert, Y. Asano, *FEBS J.* **2018**, *285*, 313–324.

[26] X. Yang, T. Matsui, T. Kodama, T. Mori, X. Zhou, F. Taura, H. Noguchi, I. Abe, H. Morita, *FEBS J.* **2016**, *283*, 1088–1106.

[27] T. Grocholski, H. Koskiniemi, Y. Lindqvist, P. Mäntsälä, J. Niemi, G. Schneider, *Biochem.* **2010**, *49*, 934–944.

[28] a) H. Li, A. D. Robertson, J. H. Jensen, *Proteins* **2005**, *61*, 704–721; b) D. C. Bas, D. M. Rogers, J. H. Jensen, *Proteins* **2008**, *73*, 765–783.

[29] K. E. Ranaghan, J. E. Hung, G. J. Bartlett, T. J. Mooibroek, J. N. Harvey, D. N. Woolfson, W. A. van der Donk, A. J. Mulholland, *Chem. Sci.* **2014**, *5*, 2191–2199.

[30] G. M. Morris, R. Huey, W. Lindstrom, M. F. Sanner, R. K. Belew, D. S. Goodsell, A. J. Olson, *J. Comput. Chem.* **2009**, *30*, 2785–2791.

[31] a) G. Candiano, M. Bruschi, L. Musante, L. Santucci, G. M. Ghiggeri, B. Carnemolla, P. Orecchia, L. Zardi, P. G. Righetti, *Electrophoresis* **2004**, *25*, 1327–1333; b) F. M. Davidson, C. Long, *Biochem. J.* **1958**, *69*, 458–466; c) H. Sato, T. Watanabe, Y. Sagane, Y. Nakazawa, K. Takano, *Food Sci. Technol. Res.* **2000**, *6*, 29–33; d) A. Shevchenko, M. Wilm, O. Vorm, M. Mann, *Anal. Chem.* **1996**, *68*, 850–858; e) D. N. Perkins, D. J. Pappin, D. M. Creasy, J. S. Cottrell, *Electrophoresis* **1999**, *20*, 3551–3567; f) M. C. Chambers, B. Maclean, R. Burke, D. Amodei, D. L. Ruderman, S. Neumann, L. Gatto, B. Fischer, B. Pratt, J. Egertson, K. Hoff, D. Kessner, N. Tasman, N. Shulman, B. Frewen, T. A. Baker, M. Y. Brusniak, C. Paulse, D. Creasy, L. Flashner, K. Kani, C. Moulding, S. L. Seymour, L. M. Nuwaysir, B. Lefebvre, F. Kuhlmann, J. Roark, P. Rainer, S. Detlev, T. Hemenway, A. Huhmer, J. Langridge, B. Connolly, T. Chadick, K. Holly, J. Eckels, E. W. Deutsch, R. L. Moritz, J. E. Katz, D. B. Agus, M. MacCoss, D. L. Tabb, P. Mallick, *Nat. Biotechnol.* **2012**, *30*, 918–920; g) D. Kessner, M. Chambers, R. Burke, D. Agus, P. Mallick, *Bioinformatics* **2008**, *24*, 2534–2536; h) B. C. Searle, *Proteomics* **2010**, *10*, 1265–1269; i) W. Kabsch, *Acta Crystallogr. Sect. D* **2010**, *66*, 125–132; j) P. Evans, *Acta Crystallogr. Sect. D* **2006**, *62*, 72–82; k) G. Winter, *J. Appl. Crystallogr.* **2010**, *43*, 186–190; l) A. Vagin, A. Teplyakov, *J. Appl. Crystallogr.* **1997**, *30*, 1022–1025; m) P. Emsley, K. Cowtan, *Acta Crystallogr. Sect. D* **2004**, *60*, 2126–2132; n) G. N. Murshudov, A. A. Vagin, E. J. Dodson, *Acta Crystallogr. Sect. D* **1997**, *53*, 240–255; o) E. J. Corey, A. Venkateswarlu, *J. Am. Chem. Soc.* **1972**, *94*, 6190–6191.

Manuscript received: February 28, 2024
Accepted manuscript online: April 17, 2024
Version of record online: ■■, ■■

Research Articles

Biocatalysis

L. M. Pick, V. Oehme, J. Hartmann, J. Wenzlaff, Q. Tang, G. Grogan,* M. B. Ansorge-Schumacher* _____ **e202404105**

SilE-R and SilE-S—DABB Proteins Catalying Enantiospecific Hydrolysis of Organosilyl Ethers

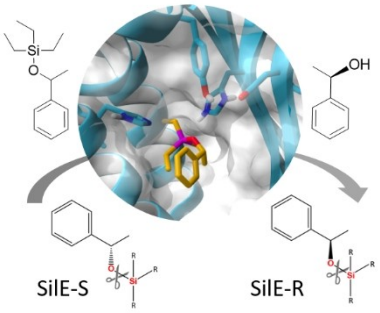

SilE–R and SilE–S, members of the DABB protein family, are the first two enzymes described that catalyse the enantiospecific hydrolysis of organosilyl ethers. They accept a wide range of substrates, including TBDMS-protected alcohols. The natural function of SilE–R and SilE–S is still unknown, but their discovery paves the way towards a green and selective transformation of organosilane organosilanol substrates.